Achieving Shape Memory: Reversible Behaviors of Cellulose–PU Blends in Wet–Dry Cycles

Hongsheng Luo,[1] Jinlian Hu,[1] Yong Zhu,[1] Sheng Zhang,[2] Ying Fan,[2] Guangdou Ye[2]

[1]*Institute of Textiles and Clothing, Faculty of Applied Science and Textiles, The Hong Kong Polytechnic University, Hung Hom, Hong Kong*
[2]*State Key Laboratory of Polymer Materials Engineering, Sichuan University, Chengdu 610065, China*

Received 30 March 2011; accepted 28 September 2011
DOI 10.1002/app.36292
Published online 26 December 2011 in Wiley Online Library (wileyonlinelibrary.com).

ABSTRACT: Shape memory effect (SME) was achieved for cellulose–polyurethane (PU) blends of different compositions in wet–dry cycles, featuring that the amorphous cellulose and the PU content served as the fixing phase and the recovery phase, respectively. The dependence on the compositions of the fixity ratio and the recovery ratio was quantitatively measured by tensile tests. The morphological and thermal properties of the blends were further investigated by scanning electron microscopy and thermogravimetric analysis. The storage modulus of the blends varied reversibly in the wet–dry cycles, as determined by dynamic mechanical analysis. Furthermore, the microstructure of the blends reversibly changed correspondingly, as determined by wide-angle X-ray scattering diffraction and Fourier transform infrared. It was predicted that the reversible transition in different amorphous cellulose structures triggered by water led to the reversible variation in modulus as well as the wet–dry SME of the blends. © 2011 Wiley Periodicals, Inc. J Appl Polym Sci 125: 657–665, 2012

Key words: cellulose; polyurethane; blends; reversible; shape memory; wet; dry

INTRODUCTION

Cellulose-synthetic polymer blends offer the promise to produce new materials with synergistic improvements in physical, physicochemical, and functional properties. Over the last few decades, blends of cellulose with various types of synthetic polymers have been investigated widely, such as cellulose with poly(ethylene glycol),[1] polyamide 66,[2] poly(vinyl alcohol),[3] and polyacrylonitrile.[4] For the preparation of cellulose blends, natural raw cellulose and synthetic polymer were dissolved into solution individually, followed by mixing the two solutions homogeneously at a desired ratio. The cellulose blends were then produced from the resultant mixture solution by coagulation method. *N*,*N*-dimethylacetamide/lithium chloride (DMAc/LiCl), as one of the most effective cellulose solvents, was widely used to prepare the cellulose-synthetic polymer blends.[5,6] Because of lack of stress in the coagulation process, the regenerated cellulose in the blends was retained in noncrystalline structure. Multiple factors, including the preparation process, individual characteristics of the mixed polymers, and the interactions between the two component polymers put dramatic influence on the final properties of the obtained blends.

Shape memory polymers (SMPs) are a very important set of polymers, which have been catching extensive academic and industrial interests for several decades. One of the most prominent characteristics of the SMPs is their capacity of fixing a temporary shape, which returns to the original shape upon exposure to external stimulus.[7,8] Different kinds of SMPs have been developed, some of which have been commonly used in industrial applications, for example, segmented polyurethane (PU).[9,10] The novel SMPs reported in the recent years include polymer blends containing elastomer styrene–butadiene–styrene triblock copolymer and switch polymer poly(ε-caprolactone),[11] chemically cross-linked acrylate polymer networks,[12] supramolecular PU with pyridine,[13] and polymer networks containing reversible quadruple hydrogen-bonding side groups.[14] However, there is very little literature on SMPs derived from cellulose, except for cellulose acetate derivatives modified with SH-group reported by Aoki et al. in 2007.[15] The cellulose derivatives developed by Aoki is solely limited to be redox

Correspondence to: J. Hu (tchujl@inet.polyu.edu.hk).
Contract grant sponsor: Hong Kong Research Grants Council Project; contract grant number: RGC-GRF/518209.
Contract grant sponsor: Hong Kong ITF Research Project; contract grant numbers: GHS/088/04, GHP/045/07TP.
Contract grant sponsor: Niche Area Fund of Hong Kong Polytechnic University; contract grant number: J-BB6M.
Contract grant sponsor: Opening Project of State Key Laboratory of Polymer Materials Engineering, Si Chuan University, China; contract grant number: 200803.

responsive. Given the hydrophilic property of cellulose in amorphous state, shape memory polymeric material based on cellulose responsive to water, rather than other stimulus, may be achievable by facile blending method. To ensure enough elasticity essential to the shape recovery, PU, an elastomer commonly used in industry, was chosen to form the blends with cellulose. This work presents the first investigation on the reversible behaviors of the cellulose–PU blends in wet–dry cycles. A heterogeneous architecture model is further proposed to explain the reversible behaviors of the blends. The finding may be beneficial to extend the potential application of cellulose in smart materials field.

EXPERIMENTAL

Materials

The raw resource of cellulose was a softwood pulp consisting of cellulose with a weight–average molecular weight of 9.82×10^5. Thermal plastic PU chips [1.06–1.15 g/mL, 330–600 K (GPC-Mw/PMMA)], synthesized with MDI (diphenyl methene-4′4′ diisocyanate), PTMG (poly tetramethylene ether glycol), and BDO (1,4-butanediol), came from Hong Kong Hi-Tech Enterprises. DMAc (anhydrous, 99.8%), obtained as HPLC grade, was used without further purification. LiCl (Merck), obtained as p.a. grade, was dried under vacuum at 180°C for 1 day before use.

Preparation of cellulose–PU blends

Homogeneous cellulose solution in DMAc/LiCl was prepared upon the previous literature.[5,6] The preparation process was briefly described as follows: pulp cellulose cut into small pieces was activated in DMAc at 150°C for 30 min. Afterward, the activated cellulose pieces were filtered and stirred in DMAc in the presence of LiCl at 90°C for 2 h under nitrogen atmosphere. The mixture was cooled down to the room temperature. Homogeneous cellulose solution was generated by keeping stirring at the room temperature for 10 h.

Blends of cellulose and PU were prepared by mixing the two contents solution under stirring at the aid of ultrasonic treatment and coagulating the mixture with ethanol and water. For the complete removal of residual DMAc and Li^+, the blend films were used in a 2-day washing process.[16] The obtained blends in the desired cellulose/PU weight ratio of 9/1, 6/1, 4/1, and 2/1 were coded as CP91, CP61, CP41, and CP21 in turn. For reference, neat samples of cellulose and PU, coded as rC and PU, were prepared as well.

Characterization of structure

Fourier transform infrared (FTIR) spectra of the samples were obtained in the wave number range of 4000–650 cm^{-1} using a Perkin-Elmer System 2000 FTIR spectrophotometer.

Wide-angle X-ray scattering diffraction (WXRD) patterns of the samples were carried out on an X-ray diffractometer (Rigaku RINT 2200V). The diffraction intensity of Cu Kα radiation (wavelength of 0.1542 nm, under a condition of 40 kV and 30 mA) was measured in a 2θ range between 5° and 40°.

A JEOL JSM-6490 scanning electronic microscopy (SEM) instrument was used to investigate the fracture surface morphology of the samples. Before the investigation, the samples were frozen and broken in liquid nitrogen. The cross section was coated with gold on JEOL JFC-1100E ion sputter coater. The SEM micrographs were obtained by using 7 kV secondary electrons.

Thermal property

Samples in the swollen state were gently pressed between two issues to remove extra water. Thermogravimetric analysis (TGA, Netzsch STA449C) for the samples was carried out in the range 30 to 200°C at the rate of 10°C per minute with Argon as the purge gas.

Mechanical properties

Dynamic mechanical analysis (DMA) of the samples was performed by using a Perkin–Elmer instrument at a frequency of 2 Hz. The size of the samples was 15 mm × 10 mm × 1 mm (length × width × height). The modulus variation of the samples in the states of wet and dry was measured. Dry-state samples were used at the beginning of the tests, which were transferred into wet state by immersion into water for 8–10 min. Reversibly, the wet-state samples were transferred into partially dry state in predefined thermal program (heating from room temperature to 90°C within 8–10 min).

Cyclic tensile tests were performed by using an INSTRON 5566 universal tensile tester equipped with a temperature control chamber. The size of the samples for the tensile tests was 20 mm length, 5 mm width, and 1 mm distance between two clamps. Wet-state samples were extended by 10% elongation (ε_m) at 10 mm/min. Afterward, the extension was fixed when the samples were transferred into the dry state in a suitable heating program. The strain was released from ε_m to 0 in an unloading procedure. After that, the wet–dry recurrent process was started. Two parameters, defined to characterize the shape memory effect (SME), fixity ratio (R_f), and recovery ratio (R_r), were determined as the formulas given below,

$$R_f = \frac{\varepsilon_u}{\varepsilon_m} \times 100\%$$

$$R_r = \frac{\varepsilon_m - \varepsilon_p}{\varepsilon_m} \times 100\%$$

where ε_m represents the maximum strain in the cyclic tensile testing, ε_u is the residual strain after

unloading in the dry state, and ε_p *is* the residual strain values of the two successive tensile cycles after shape recovery.

RESULTS AND DISCUSSION

Preparation and morphologies of the blends

Figure 1 shows the molecular structures of cellulose and PU. The mixing solution of cellulose and PU was visibly homogeneous. The obtained blend films coagulated from ethanol and water were transparent and gel-like in appearance. However, it was difficult to form visibly homogeneous films when the PU content was more than 50 wt % in the blends. Therefore, all the blend samples were designed to contain cellulose as the prominent content in this work. The blends gradually lost their transparency and became increasingly heterogeneous under heat treatment from room temperature to 90°C, indicating that phase separation occurred in the blends. The SEM images of the blends are shown in Figure 2. It was found that cellulose and PU were partially miscible in microscale. Compared to the morphologies of the blends in different compositions, the blends decreased the homogeneity with the increase of the PU content. Obvious phase separation was absent for CP91. However, CP41 and CP21 had microscale PU aggregates embedded in the cellulose matrix. The similar heterogeneous morphology was observed in other cellulose-synthetic polymer systems as well. For instance, polyamide formed domains appeared like "marbles" or beads, whose size and distribution were very irregular, embedded in an amorphous cellulose matrix in cellulose/

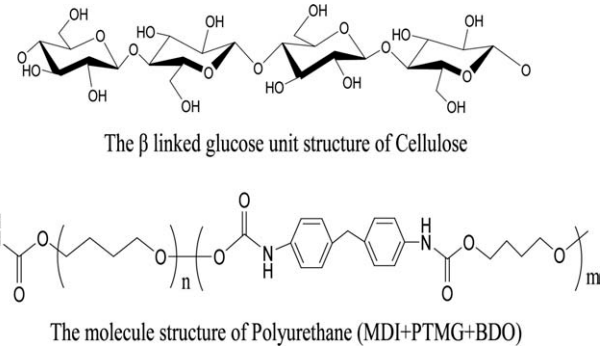

Figure 1 Molecular structures of cellulose and PU.

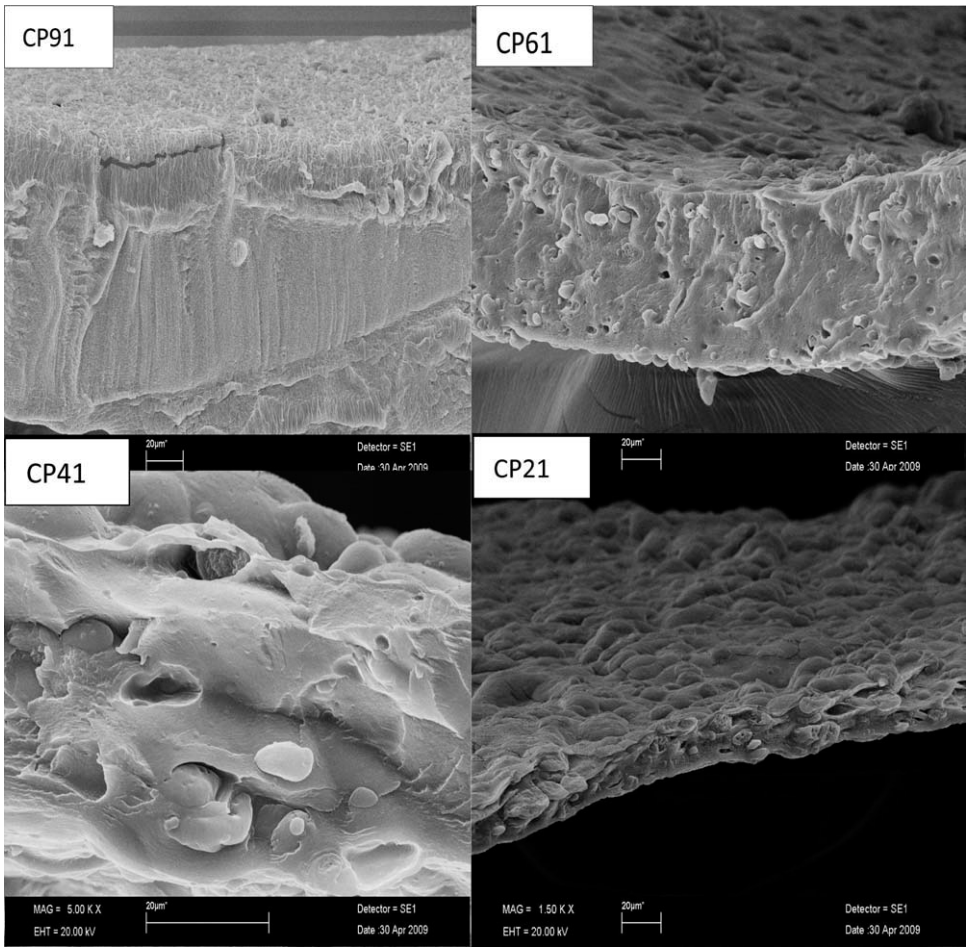

Figure 2 SEM images of cellulose-PU blends in different compositions.

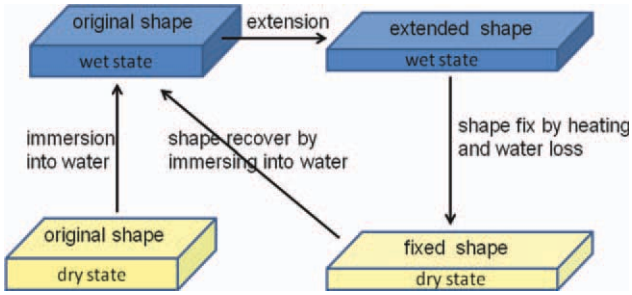

Scheme 1 Illustration of the wet-dry shape memory cycle for the cellulose-PU blends. [Color figure can be viewed in the online issue, which is available at wileyonlinelibrary.com.]

polyamide blends[17]; cellulose/poly(vinyl pyrrolidone) blends also showed two-phase-separated structure where cellulose served as a continuous matrix.[18]

SME of the blends in the wet–dry cycles

Intrigued by the thermally induced shape memory procedure, a wet–dry cycle was explored for the cellulose–PU blends, typically containing three steps described as follows (Scheme 1): first, the blends swollen by water (wet state) were extended by 10% under external force; second, the extended blends were heated from the room temperature to 90°C within 8–10 min (partially dry state). The extension was gradually fixed due to the water loss; third, the fixed blends recovered to their original shape by dropping water on the blends to swell (wet state).

The reason that the maximum extension was defined to be 10% was to avoid possible irreversible part of the large-scale deformation in the blends. The heating program for the shape fixing was determined upon the results of TGA tests (shown in Fig. 3). All the wet-state samples rapidly decreased their weights in the temperature range 50–120°C. When the temperature reached to 200°C, neat sample rC had the greatest percentage of weight loss of around 60%, whereas CP21 had the least of 28%. The results indicated that the amorphous cellulose content, instead of the PU in the blends, contributed to the primary water absorption. Furthermore, arising the temperature from room temperature to around 90°C was found ensuring all the swollen samples lose more than 50% of the water content. The TGA curves provided necessary reference to determine the heating program used to realize the state transition for the blend samples from swollen state toward partially dry state, which allowed the shape fixing. As a result, the temperature program that heating from the room temperature to 90°C within 8–10 min was applied in the wet–dry shape memory cyclic measurements.

The wet–dry SME of the cellulose–PU blends were quantitatively measured by tensile tests. Figure 4 shows the stress–strain curves of the neat sample rC and the four blend samples. The two parameters to assess the SME, R_f and R_r, were calculated correspondingly. Figure 5 shows the dependence of the R_f and the R_r on the compositions of the blends. The blends had lower R_f and higher R_r with the increase of the PU content. Sample rC had the highest R_f of 93% and the lowest R_r of 52%. By contrast, CP21 had the lowest R_f of 55% and the highest R_r of 95%. The variation in R_f and R_r against the compositions provided strong evidence that cellulose and PU played different role for the wet–dry SME of the blends. Speaking in detail, the cellulose content was responsible for the shape fixing, whereas the PU content was responsible for the shape recovery. The former served as fixing phase, which can be triggered by water reversibly, while the latter served as recovery phase providing sufficient elasticity for the shape recovery. Increase of the PU content made relatively higher R_r achievable, meanwhile, led to lower R_f. The weight ratio of 5/1 was predicted to be an optimized composition, ensuring that the blends obtain a balance between the R_f and R_r both of which were more than 80%.

Dynamic mechanical analysis of the blends in the wet–dry cycles

Modulus variation under external stimulus was prerequisite for polymers to achieve SME.[8,19–21] To further characterize the SME of the cellulose–PU blends, DMA measurements were performed for the blends in wet–dry cycles. Figures 6 and 7 show the dependence on time of the storage modulus E' of the neat samples and the blends in the wet–dry cycles. All the samples experienced the wet–dry cycles for three times, including three times of heating and swelling. The dashed lines were used to separate the heating and swelling periods in the

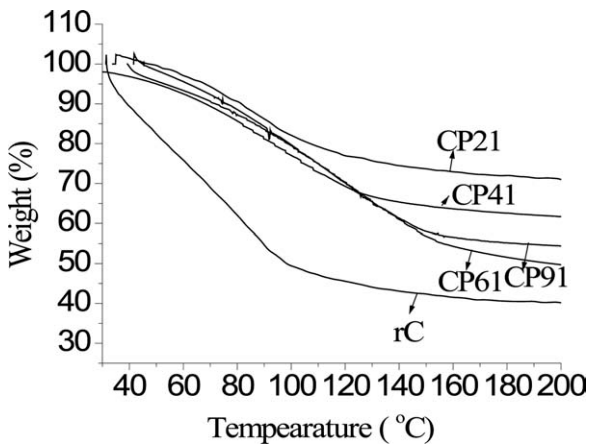

Figure 3 Thermogravimetric analysis of cellulose-PU blends.

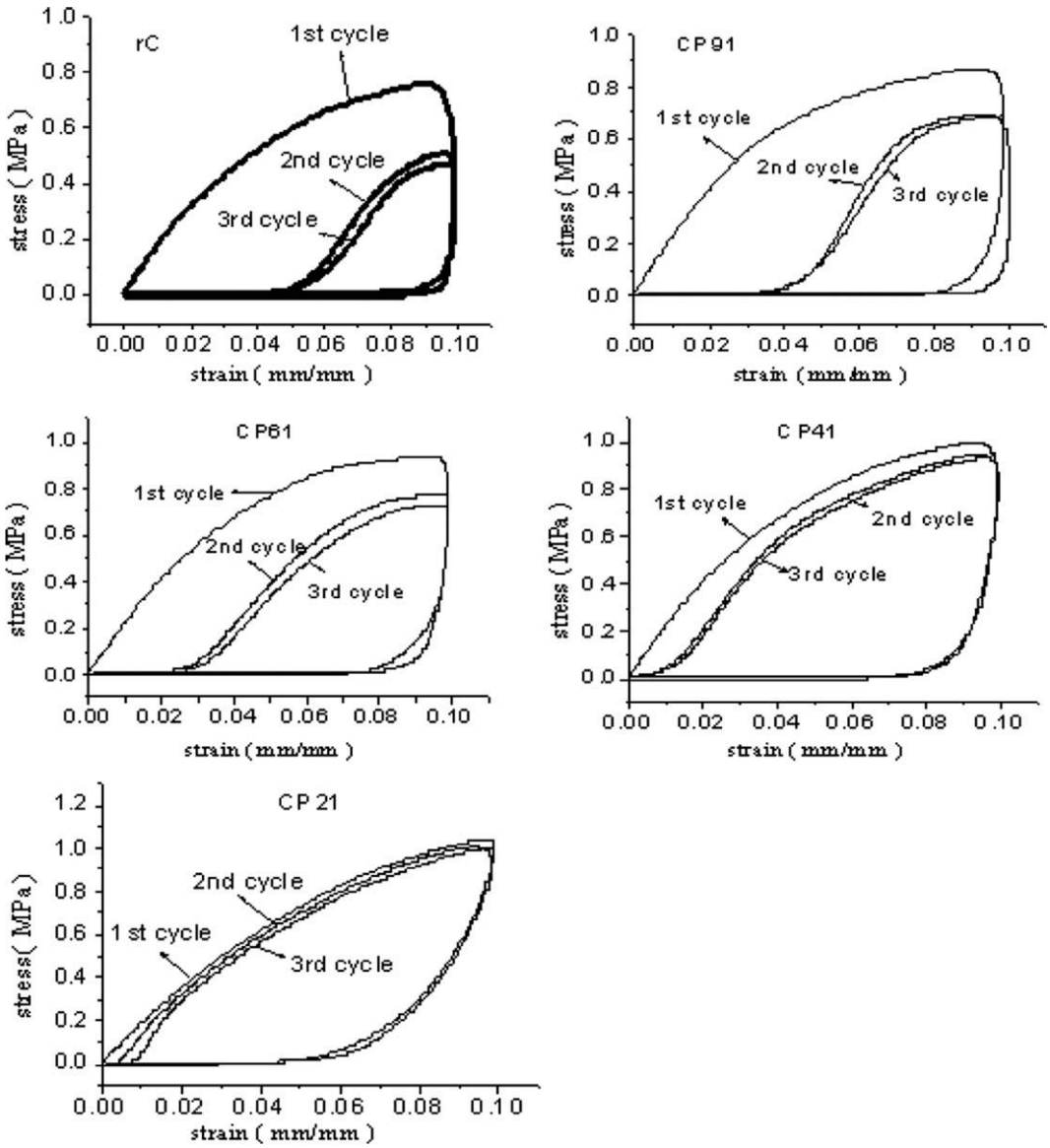

Figure 4 Cyclic stress–strain curves of the neat sample rC and the blends.

figures. The modulus of the wet–state blends was as low as near 1 MPa in the beginning of the tests. Subsequently, the modulus gradually increased, reached around 6 MPa when the samples were heated up to 90°C from the room temperature. The increased modulus of the blends fell to near 1 MPa by immersing into water. Except for the neat cellulose sample rC, all the blend samples exhibited reversible modulus variation between near 1 MPa and near 6 MPa in the cyclic state transition of wet and dry.

The modulus contrast of the samples in the wet and the dry states was affected by the sample compositions. Neat cellulose sample rC had the minimum modulus contrast of around two, whereas the blend samples had around six. Furthermore, for the dry-state blends, the addition of the PU content pronounced increased the modulus. For instance, the maximum modulus of the neat sample rC in the dry state was around 2 MPa, while it was enhanced to more than 5 MPa when the PU content was added.

Reversible variation in microstructure of the blends in the wet–dry cycles

The WXRD profiles of the raw material and the neat samples, including the cellulose pulp, rC, and PU, are shown in Figure 8. A broad diffraction peak located at 19.69° for PU and three obvious peak signals located at 9.0°, 17.83°, and 20.08° for cellulose pulp. It was reported that the crystalline scatter of 22.5° for cellulose I or of 19.8° for cellulose II as well as the amorphous reflection of 18° for cellulose I or 16° for cellulose II, respectively.[22–24] Therefore, the broad peak of the cellulose pulp in the range 18°

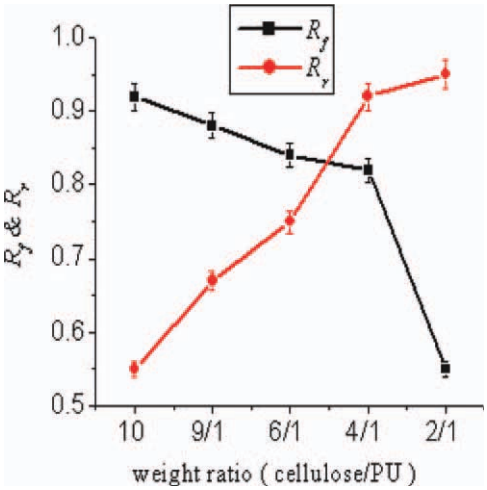

Figure 5 Dependence of R_f and R_r on compositions of the cellulose-PU blends. [Color figure can be viewed in the online issue, which is available at wileyonlinelibrary.com.]

and 22° can be assigned to the combined amorphous-crystalline structures in the pulp. In comparison with the cellulose pulp, the diffraction peaks due to crystalline structure nearly disappeared for rC in both wet and dry states, indicating that the crystalline structure in the cellulose pulp was disrupted fully in the process of dissolution and coagulation. Figure 9 shows the WXRD profiles of blends CP91, CP61, CP41, and CP21 in the wet and the dry states. Although sharp peaks due to the crystalline structure were absent in all the profiles of the blends, broad diffraction peaks were observed at near 27° for the wet-state blends. In particular, the broad diffraction peaks became much sharper and shifted to near 20° from 27° when the blends were transferred into the dry states. Immersion of the

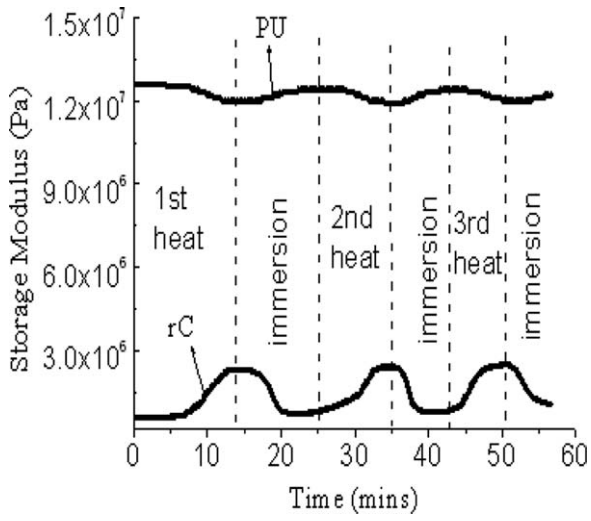

Figure 6 Variation in storage modulus of rC and PU against time in wet-dry cycles determined by DMA.

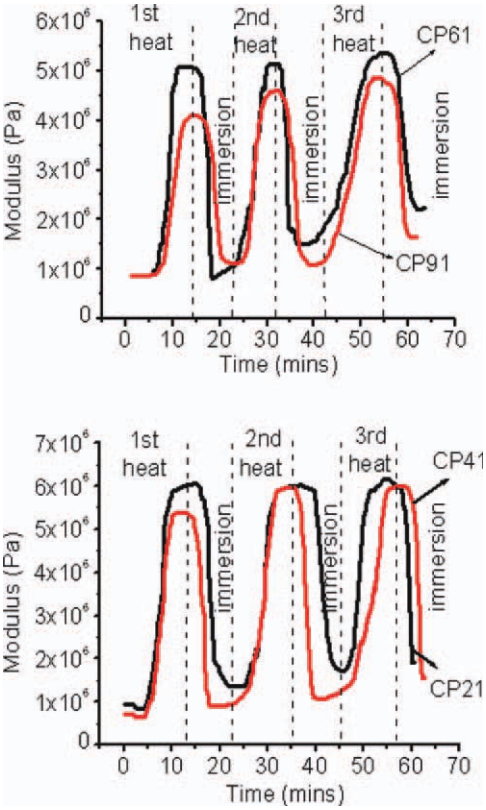

Figure 7 Variation in storage modulus of the blends against time in wet-dry cycles determined by DMA. [Color figure can be viewed in the online issue, which is available at wileyonlinelibrary.com.]

blends into water again resulted into the diffraction peaks shifted back to the locations at higher degree. Meanwhile, the intensity of the peaks was decreased correspondingly. The variation in the location and the intensity of the diffraction peaks indicated that some changes in the microstructures of the blends occurred during state transition between the wet and the dry states. In general, the partially dry-state blends had much compact microstructure compared to the wet-state blends in the almost fully

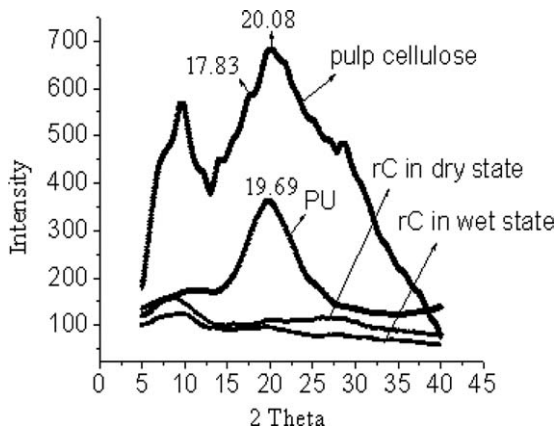

Figure 8 WXRD profiles of rC and pulp cellulose.

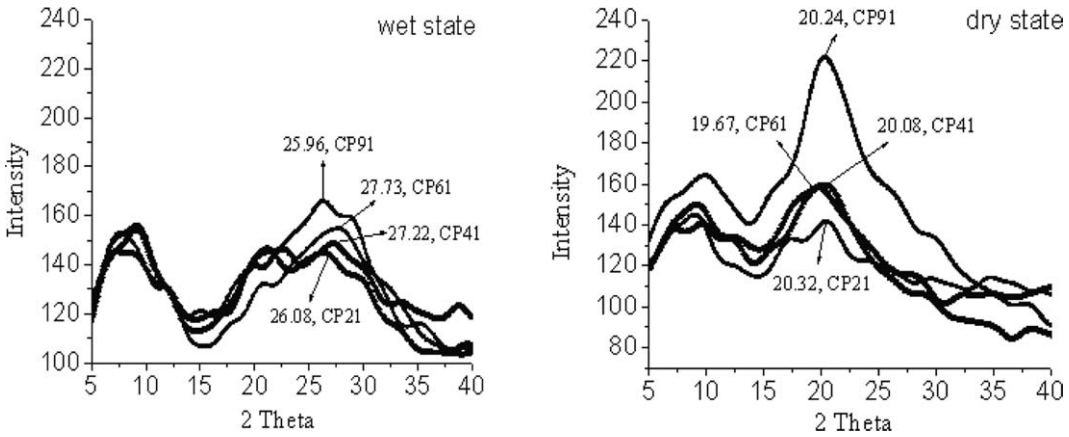

Figure 9 WXRD profiles of the blends in the wet (left) and the dry (right) states.

amorphous structure. The variation in the microstructure of the blends was further investigated by FTIR method. Figures 10 and 11 show the FTIR spectrum in the range 1600 cm^{-1} and 800 cm^{-1} for the neat samples and the blends in the wet and the dry states. Obvious absorption peaks appeared for PU and rC in Figure 10. It seemed that water had little influence on the absorption of the PU. On the other hand, the rC exhibited significant difference on the absorptions according to the states. The dry-state rC had much intensive peak located at 1427 cm^{-1} and less intensive peak located at 895 cm^{-1} compared to the wet-state rC. The similar phenomenon was observed for the blends in Figure 11. When the blends were transferred into the dry state from the wet state, the absorption band locating at 1427 cm^{-1} increased; meanwhile, the band locating at 895 cm^{-1} decreased remarkably. Natural cellulose was well known for the polymorphs. The absorbance intensities in the range 1427–1430 cm^{-1} as well as in the range 987–893 cm^{-1} were very sensitive to the amount of crystalline versus amorphous structure.[25–27]

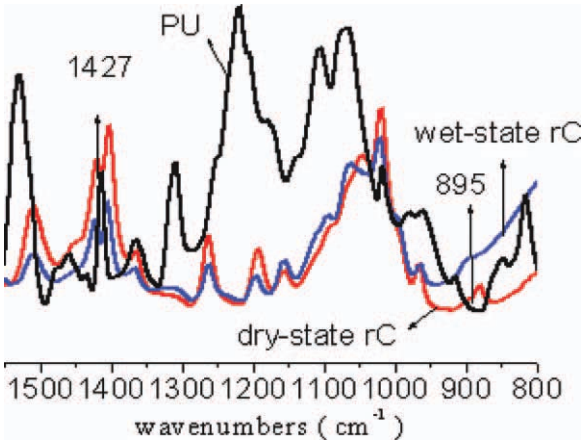

Figure 10 FTIR spectrum of the neat samples rC and PU. [Color figure can be viewed in the online issue, which is available at wileyonlinelibrary.com.]

To analyze the microstructure changes of the cellulose–PU blends in the wet-dry cycles quantitatively, a combined compact index (CCI) for the blends was defined as the absorbance ratio of the bands at 1427 and 895 cm^{-1}. The calculation formula is shown as below,

$$\mathrm{CCI} = \frac{A_{1427\ \mathrm{cm}^{-1}}}{A_{895\ \mathrm{cm}^{-1}}}$$

Figure 12 shows the curves of CCI against compositions for the wet-state and the dry-state blends. All the blend samples increased CCI up to 2.0–3.2 in the dry state while decreased the index to 0.8–1.2 in the wet state. Both the dry-state and the wet-state blends slightly decrease the CCI with the increase of the PU content. rC in the dry state had the maximum value of 3.2, whereas CP21 in the wet-state had the minimum value of 0.5. Given the deformation was fixed for the dry-state blends as well as the shape was recovered for the wet-state blends in the shape memory cycles, this phenomenon was consistent with the tensile results that rC and CP21 obtained the best fixity ratio and the recovery ratio, respectively. The FTIR measurement not only disclosed that the dry-state blends had much compact structure near to the crystalline structure compared to the wet-state blends, but also revealed that the structure changes of blends in the wet–dry cycles primarily attributed to the cellulose, rather than PU. The FTIR results coupled with the observation using WXRD provided strong evidence on the variation in the microstructures of the blends, which laid important foundation to disclose the underline mechanism for the wet–dry SME of the blends.

Combined heterogeneous architecture model for the cellulose–PU blends

Hishikawa et al.[28] have revealed that the noncrystalline phase of cellulose was not composed solely of

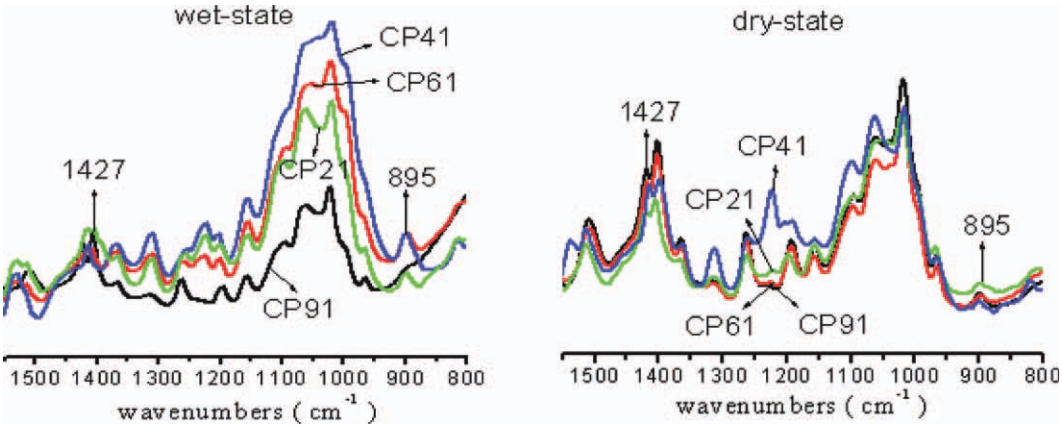

Figure 11 FTIR spectrum of the blends in the wet (left) and the dry (right) states. [Color figure can be viewed in the online issue, which is available at wileyonlinelibrary.com.]

homogeneous domains nor were they totally amorphous but rather were found to have a heterogeneous organization. Given the absence of signals assigned to the crystalline structures in the investigation on the microstructure of the blends, it was reasonable to assume that the cellulose in the blends formed different amorphous regions primarily consisting of the fully amorphous region and the compact amorphous region. A combined heterogeneous architecture model was further proposed to explain the reversible behaviors of the blends in the wet–dry cycles, which is shown in Scheme 2. The wet-state blends had a loose structure where the fully amorphous cellulose and the PU were combined. Because of the abundant hydroxyl groups of the cellulose, water was easy to diffuse into or be removed from the amorphous regions. When the blends were applied into the heating program, the fully amorphous region was reversibly transferred into a much compact architecture accompanied with the water loss. The above-mentioned results from the WXRD and FTIR measurements were predicted to support the assumption. Frantz et al.[29] have demonstrated that heat treatment could change not only the mobility of water content but also the relaxation behavior of cellulose chains. The impact of thermal and aqueous treatment on the phase behaviors of the cellulose was also reported in other literature.[30,31] The reversible transition of the cellulose in different amorphous regions provided a possible mechanism for the wet–dry SME of the blends.

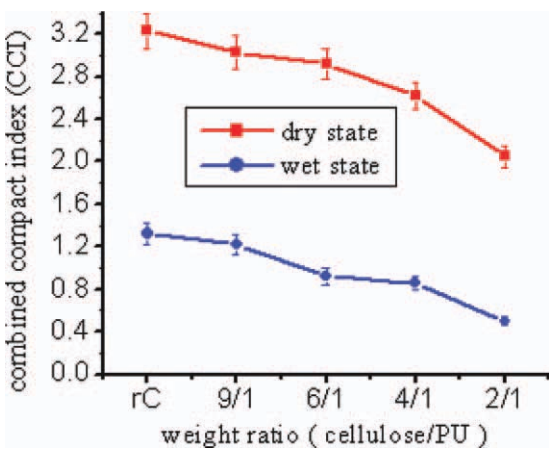

Figure 12 Dependence on compositions of CCI of the wet and the dry state samples. [Color figure can be viewed in the online issue, which is available at wileyonlinelibrary.com.]

CONCLUSIONS

Cellulose–PU blends with different compositions were prepared by coagulation method. The blends were visibly homogeneous. The two polymer contents were partially miscible in the blends. With the increase in the content ratio, PU tended to form microscale aggregates embedded in the amorphous cellulose matrix. SME was realized for the blends when applied into a specifically explored wet–dry cycle. PU content served as the recovery phase,

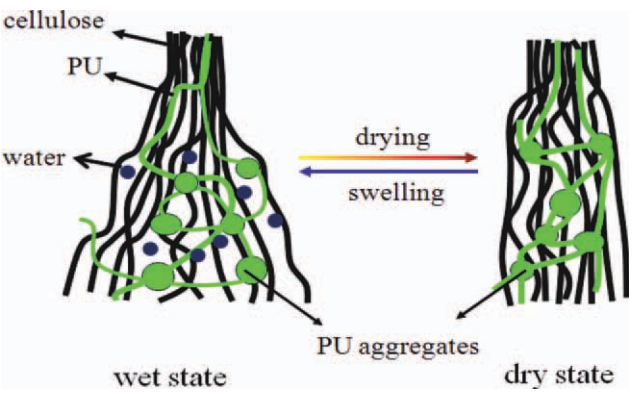

Scheme 2 Heterogeneous architecture model of the cellulose-PU blends. [Color figure can be viewed in the online issue, which is available at wileyonlinelibrary.com.]

while the cellulose content served as the fixing phase in the blends. The modulus and the microstructure of the blends varied reversibly in the wet–dry cycles. The cellulose was able to arrange into different types of amorphous structures including a fully amorphous structure and a much compact structure according to the wet or dry state of the blends. Water can be absorbed or removed from the amorphous cellulose structures, resulting into the reversible variation in the microstructure of the blends as well as the wet–dry SME.

References

1. Shen, Q.; Liu, D. S. Carbohydr Polym 2007, 69, 293.
2. Ramirez, M. G.; Cavaille, J. Y.; Dufresne, A.; Tekely, P. J Polym Sci Part B: Polym Phys 2003, 33, 2109.
3. Radloff, D.; Boeffel, C.; Spiess, H. Macromolecules 1996, 29, 1528.
4. Baalbaki, Z.; Prudhomme, R. E. J Appl Polym Sci 1979, 24, 887.
5. Dupont, A. L. Polymer 2003, 44, 4117.
6. Marson, G. A.; El Seoud, O. A. J Polym Sci Polym Chem 1999, 37, 3738.
7. Huang, W. M.; Yang, B.; Zhao, Y.; Ding, Z. J Mater Chem 2010, 20, 3367.
8. Mather, P. T.; Luo, X. F.; Rousseau, I. A. Annu Rev Mater Res 2009, 39, 445.
9. Hu, J. L.; Ji, F. L.; Wong, Y. W. Polym Int 2005, 54, 600.
10. Lee, B. S.; Chun, B. C.; Chung, Y. C.; Sul, K. I.; Cho, J. W. Macromolecules 2001, 34, 6431.
11. Zhang, H.; Wang, H. T.; Zhong, W.; Du, Q. G. Polymer 2009, 50, 1596.
12. Safranski, D. L.; Gall, K. Polymer 2008, 49, 4446.
13. Chen, S.; Hu, J.; Zhuo, H.; Yuen, C.; Chan, L. Polymer 2010, 51, 240.
14. Li, J. H.; Viveros, J. A.; Wrue, M. H.; Anthamatten, M. Adv Mater 2007, 19, 2851.
15. Aoki, D.; Teramoto, Y.; Nishio, Y. Biomacromolecules 2007, 8, 3749.
16. Nayak, J. N.; Chen, Y.; Kim, J. Ind Eng Chem Res 2008, 47, 1702.
17. Garciaramirez, M.; Cavaille, J. Y.; Dupeyre, D.; Peguy, A. J Polym Sci Polym Phys 1994, 32, 1437.
18. Paillet, M.; Cavaille, J. Y.; Desbrieres, J.; Dupeyre, D.; Peguy, A. Colloid Polym Sci 1993, 271, 311.
19. Lendlein, A.; Schmidt, A. M.; Langer, R. Proc Natl Acad Sci USA 2001, 98, 842.
20. Tobushi, H.; Ito, N.; Takata, K.; Hayashi, S. Shape Memory Mater 2000, 327–323, 343.
21. Madbouly, S. A.; Lendlein, A. Adv Polym Sci 2010, 226, 41.
22. Zhao, H. B.; Kwak, J. H.; Zhang, Z. C.; Brown, H. M.; Arey, B. W.; Holladay, J. E. Carbohydr Polym 2007, 68, 235.
23. Mansikkamaki, P.; Lahtinen, M.; Rissanen, K. Cellulose 2005, 12, 233.
24. Moharram, M. A.; Mahmoud, O. M. J Appl Polym Sci 2007, 105, 2978.
25. Oh, S. Y.; Yoo, D. I.; Shin, Y.; Seo, G. Carbohydr Res 2005, 340, 417.
26. Kondo, T. Cellulose 1997, 4, 281.
27. Carrillo, A.; Colom, X.; Sunol, J. J.; Saurina, J. Eur Polym J 2004, 40, 2229.
28. Hishikawa, Y.; Togawa, E.; Kataoka, Y.; Kondo, T. Polymer 1999, 40, 7117.
29. Frantz, S.; Hubner, G. A.; Wendland, O.; Roduner, E.; Mariani, C.; Ottaviani, M. F.; Batchelor, S. N. J Phys Chem B 2005, 109, 11572.
30. Suchy, M.; Kontturi, E.; Vuorinen, T. Biomacromolecules 2010, 11, 2161.
31. Suchy, M.; Virtanen, J.; Kontturi, E.; Vuorinen, T. Biomacromolecules 2010, 11, 515.